Accepted Manuscript

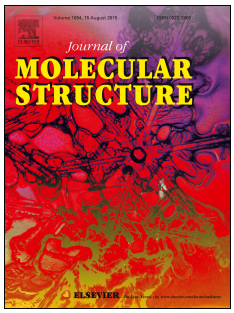

Density functional theory study of carbazole dyes: Potential application of carbazole dyes in dye-sensitized solar cells

Alireza Salimi Beni, Maryam Zarandi, Behzad Hosseinzadeh, A. Najafi Chermahini

PII: S0022-2860(18)30248-5

DOI: 10.1016/j.molstruc.2018.02.094

Reference: MOLSTR 24916

To appear in: *Journal of Molecular Structure*

Received Date: 2 October 2017

Revised Date: 25 January 2018

Accepted Date: 24 February 2018

Please cite this article as: A. Salimi Beni, M. Zarandi, B. Hosseinzadeh, A. Najafi Chermahini, Density functional theory study of carbazole dyes: Potential application of carbazole dyes in dye-sensitized solar cells, *Journal of Molecular Structure* (2018), doi: 10.1016/j.molstruc.2018.02.094.

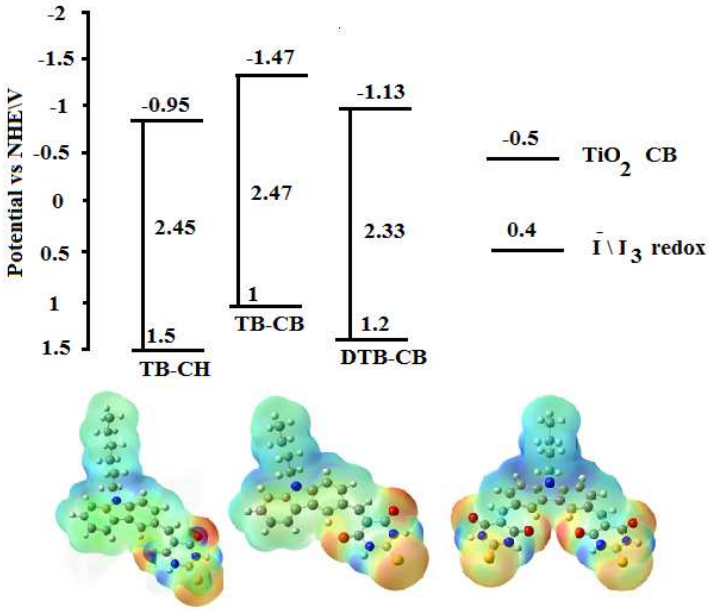

Density functional theory study of carbazole dyes: potential application of carbazole dyes in dye-sensitized solar cells

Alireza Salimi Beni[a]*, Maryam Zarandi**[b], Behzad Hosseinzadeh[c], A. Najafi Chermahini[d]

[a] Department of Chemistry, Faculty of Science, Yasouj University, Yasouj, 75918-74831, Iran

[b] Young Researchers and Elite Club, Qom Branch, Islamic Azad University, Qom, Iran

[c] Department of Chemistry, Mazandaran University, Babolsar, Iran

[d] Department of Chemistry, Isfahan University of Technology, Isfahan 84156-83111, Iran

*Tel: +98 741 2223048, fax: +98 741 3342172

*E-mail: salimibeni@mail.yu.ac.ir

**E-mail: Maryam.zarandi88@gmail.com

Abstract: Dyes applied in dye synthesized solar cells are an important class of organic compounds. In order to extension novel dyes, three organic dyes (TB-CH, TB-CB and DTB-CB) which contain hexyl and butyl moieties as a branch and thiobarbutiric acid moiety as an electron acceptor, connected by carbazole unit have been studied. We report the synthesis, molecular structures, and study of adsorption of dyes on TiO_2 anatase by density functional theory (DFT). Molecular orbital analysis study indicated all dyes can give suitable electron injection from their LUMO orbitals to the TiO_2 conduction band. Also, dyes were investigated by UV spectroscopy and cyclic voltammetry (CV). The synthesized dyes were characterized extensively by IR, ^{1}HNMR, ^{13}CNMR, mass spectroscopy and CHN analysis. Results of Photo physical, electrochemical properties and density functional theory investigation indicated TB-CH, TB-CB and DTB-CB have potential for application in dye sensitized solar cell. The adsorption energy of each dye/TiO_2 complex was -1.05, -1.01 and -1.00 eV for TB-CH, TB-CB and DTB-CB, respectively.

Keyword: Organic dye, Carbazole, Density functional theory, Dye sensitized solar cell

1. Introduction

One of the important demands in all over world is to find renewable energy sources. Therefore developing solar cells is one of the important researchers aim. In 1991 Grätzel and co-workers have been developed third generation of solar cells, namely nanocrystalline dye-sensitized solar cell (DSSC) [1-3]. Dye sensitized solar cells (DSSCs) have attracted much attention, due to their high light-to-electrical conversion efficiency, low cost, and long-term stability[4,5]. The function of DSSC usually depends to three factors: 1) the mesoporous oxide semiconductor nanoparticle layers, 2) dye sensitizers, which attached to the surfaces of the oxide semiconductors and 3) electrolyte that is the medium containing redox system. The fundamental concept of DSSC function is based on photon to current conversion mechanism. Sunlight passes through the transparent electrode into the dye layer where it can excite electrons that then flow into the titanium dioxide. The electrons flow toward the transparent electrode where they are collected for powering a load. After flowing through the external circuit, they are re-introduced into the cell on a metal electrode on the back, flowing into the electrolyte. The electrolyte then transports the electrons back to the dye molecules. [6]. Up to now different scientist focused on design and developing dye-sensitized solar cells. Therefore different metallic and organic dyes have been developed [7-16].

The metallic dyes have some shortcoming include: high cost, highly energy consuming method preparation, toxicity and Low natural abundance [7,8]. In order to overcome these problems new generation of dyes developed which contain no metals. One way to investigate new dyes efficiency is theoretical approach. Density functional theory (DFT) is a useful method for the theoretical treatment of molecular structures and electronic absorption spectra [17,18]. Titanium dioxide (TiO_2) has been extensively applied as a model metal oxide with a wide range of applications in catalysis, photochemistry, and electrochemistry [19]. So many academic researchers studied versatile compound adsorption on TiO_2 anatase surfaces by density functional theory [20-22].

In this study, in continues our investigation about organic compound [23-24], we report synthesis and characterization of several dyes contain thiobarbutiric acid moiety as anchoring group. We

investigate theoretical electronic structures, the optical properties and adsorption on TiO_2 anatase surfaces of dyes. Their potential for application in dye synthesized solar cells discussed.

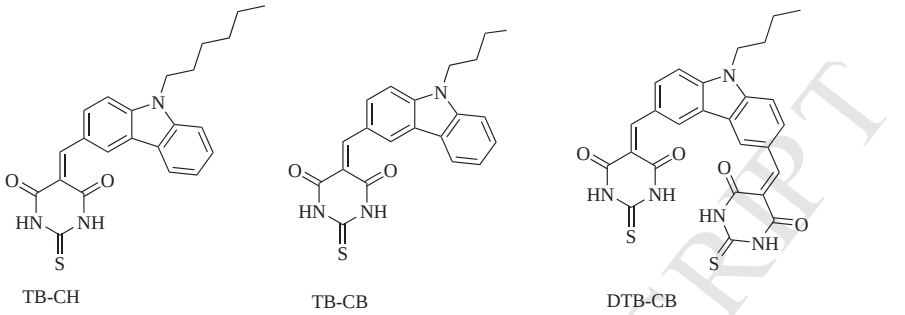

Figure 1. Chemical structure of designed and synthesized novel dyes TB-CH, TB-CB and BTD-CB

2. Experimental

2. 1.Materials and characterization

All solvents and other chemicals were reagent grade and used without further purification. All chemical were purchased from Merck and Sigma Aldrich. Melting points were measured on an elecrtothermal KSB1N apparatus. TLC was performed on TLC-Grade silica gel-G/UV 254 nm plates (*n*-hexane and ethyl acetate). ^{1}H and ^{13}CNMR spectra were recorded on a FT-NMR Bruker Advance ultra-shield spectrometer (frequency line: 400, MHz for ^{1}HNMR and 100 MHz for ^{13}C NMR; solvents, $CDCl_3$ and DMSO-d_6). FT-IR spectra were recorded in the matrix of KBr with JASCO FT-IR-680 plus spectrometer. Mass spectra of the products were obtained with a HP Agilent technologies 5937with mass selective detector. Elemental analyses (C, H, N) were performed with a Heraeus CHN-O-Rapid analyzer.

2.2. Photo physical and electrochemical measurements

Absorption spectra were measured with Perkin Elmer (Lambda 25) UV–VIS spectrophotometer. Cyclic voltammetry experiments were performed in dimethylformamide (DMF) (3.0×10^{-4} M) containing 0.1 M n-Bu_4NPF_6 as the supporting electrolyte by biologic SP 150 electrochemical analyzer with scan rate of 100 $mVs^{-1,}$ the platinum wire as counter and working electrodes and Ag/AgCl as reference electrode.

2.3. Synthesis of dyes

2.3.1. Synthesis of 9-Hexyl-9H-carbazole

In a dried 100 ml, round bottom flask carbazole (0.20 g, 1.10 mmol) were dissolved in DMSO (3 mL), NaOH (0.40 g) added and then the hexylbromide (0.33g, 1.01 mmol) was added drop wise. After complete addition, the reaction mixture was heated at 90℃ overnight. The organic layer was separated, washed three times with 50 ml water, dried over $MgSO_4$ and concentrated. Pure product was obtained after silica gel column chromatography (normal hexane) as a white solid.

White powder, yield 85%, mp = 75-77℃

IR (KBr, cm^{-1}): 3051, 2955, 2923, 2869, 2856, 1628, 1594, 1487, 1453, 1376, 1327, 1241, 1217, 1192, 1153 and 1128.

^{1}H NMR (400 MHz, $CDCl_3$, 20℃) δ (ppm): 8.13 (d, *J*=8 Hz, 2H), 7.44(m, 4H), 7.23 (t, *J*=8 Hz, 2H), 4.33 (t, *J*=7Hz, 2H), 1.88 (m, 2H), 1.33 (m, 6H) and 0.89 (t, *J*=7 Hz, 3H)

^{13}C NMR (100 MHz, $CDCl_3$, 20℃) δ (ppm): 141.3, 126.4, 123.4, 121.1, 119.4, 109.5, 43.6, 32.4, 29.6, 27.7, 23.1 and 14.8

2.3.2. Synthesis of 9-Butyl-9H-carbazole

To a stirred solution of carbazole (0.20 g, 1.1 mmol) in DMSO (3 mL), NaOH (0.40 g) was added and then the corresponding n-butylbromide (0.13g, 1.01 mmol) was added drop wise. After complete addition, the reaction mixture was heated at 90 for℃ overnight. The organic layer was separated, washed with water, dried over Na_2SO_4 and concentrated. Pure product was obtained after silica gel column chromatography (normal hexane) as a white solid.

White powder, Yield: 83%, mp: 54-55℃

FT-IR (KBr, cm^{-1}): 3043, 2953, 2928, 1918, 1625, 1591, 1482, 1463, 1348 and 1325.

^{1}HNMR (300 MHz, $CDCl_3$) (ppm): 8.23 (m, 2H), 7.54 (m, 4H), 7.39 (m, 2H), 4.45 (t, *J* = 6 Hz, 2H), 1.96 (m, 2H), 1.54 (m, 2H), 1.11 (t, *J*= 7Hz, 3H)

2.3.3. Synthesis of butyl-carbazole-3,6-dicarbaldehyde (1)

Phosphorylchloride (2.31 mL, 2.5eq) was added drop wise to DMF (1.76 mL, 2.3 eq) for 1 h at 0℃. The mixture was stirred and then N-(butyl) carbazole (0.22 g, 1 mmol) added over 1 h at room temperature. After standing for overnight at 90℃, the mixture was poured into ice–water (30 mL), stirred 5h, and neutralized with sodium hydroxide. The solution was extracted three times with ethyl acetate and dried with $MgSO_4$. The solvent was removed under reduced pressure. The residue was purified by silica gel column chromatography (eluent: ethyl acetate/ n-hexane =1:9).

Cream powder, Yield: 60%, mp: 145-150 °C.

FT-IR (KBr, cm^{-1}): 2956, 2863, 2811, 2722, 1685, 1629, 1627, 1592, 1488, 1205 and 1125.

^{1}HNMR (400 MHz, DMSO-d_6) δ (ppm): 10.94 (s, 2H), 8.88 (s, 2H), 8.79 (d, *J*= 8 Hz, 2H), 8.13 (d, *J* = 8 Hz, 2H), 4.53 (t, *J* = 12 Hz, 2H), 1.77 (m, 2H), 1.32 (m, 2H) and 0.89 (t, *J* = 1Hz, 3H). ^{13}CNMR (100 MHz, DMSO-d_6) δ (ppm): 190.9, 144.1, 128.9, 127.7, 124.6, 122.6, 110.9, 42.6, 30.8, 19.8 and 13.9.

2.3.4. 9-Butyl-9H-carbazole-3-carbaldehyde (2)

Phosphorylchloride (1.55 mL, 1.25eq) was added drop wise to N, N-dimethylformamide (DMF, 0.88 mL, 1.15 eq) for 1 h at 0℃. The mixture was stirred and then N-(butyl) carbazole (0.25 g, 1 mmol) added over 1 h at room temperature. After standing for 5 hr. at 90℃, the mixture was poured into ice–water (30 mL), stirred 5h, and neutralized with sodium hydroxide. The solution was extracted three times with ethyl acetate and dried with Na_2SO_4. The solvent was removed under reduced pressure. The residue was purified by silica gel column chromatography (eluent: ethyl acetate/ n-hexane =1:9).

Cream powder, Yield: 55%, mp: 62-64℃.

FT-IR (KBr, cm^{-1}): 2985, 1691, 1625, 1594, 1473, 1352, 1133 and 808.

^{1}HNMR (400 MHz, DMSO-d_6) δ (ppm): 10.06 (s, 1H), 8.76 (s, 1H), 8.30 (d, *J* = 8 Hz, 1H), 7.99 (m, 1H), 7.79 (d, *J* = 8 Hz, 1H), 7.70 (d, *J* = 8 Hz, 1H), 7.54 (m, 1H), 7.31 (t, *J* = 7.6 Hz, 1H), 4.46 (t, *J* = 8 Hz, 2H),1.76 (m, 2H),1.29 (m, 2H) and 0.87 (t, *J* = 8 Hz, 3H).

^{13}CNMR (100 MHz, DMSO-d_6) δ (ppm): 192.1, 142.8, 140.9, 128.7, 126.6, 124.4, 122.4, 120.9, 120.44, 110.2, 110.4, 42.7, 30.9, 19.8 and 13.3.

2.3.5. 9-Hexyl-9H-carbazole-3-carbaldehyde (3)

Phosphorylchloride (1.55 mL, 1.25eq) was added drop wise to DMF (0.88 mL, 1.15 eq) for 1 h at 0℃. The mixture was stirred and then N-(hexyl) carbazole (0.25 g, 1 mmol) added over 1 h at room temperature. After standing for 5 hr. at 90℃, the mixture was poured into ice–water (30 mL), stirred 5h, and neutralized with sodium hydroxide. The solution was extracted three times with ethyl acetate and dried with $MgSO_4$. The solvent was removed under reduced pressure. The residue was purified by silica gel column chromatography (eluent: ethyl acetate/ n-hexane =1:9).

Cream powder, Yield: 55%, mp: 70-74℃.

FT-IR (KBr, cm^{-1}): 3052, 2955, 2929, 2857, 2727, 1893, 1686, 1593, 1469, 1383, 1352, 1339, 1329, 1240, 1177, 1135, 807, 765, 748 and 730.

^{1}HNMR (400 MHz, DMSO-d_6) δ (ppm): 10.06 (s, 1H), 8.77 (s, 1H), 8.30 (d, *J* = 8 Hz, 1H), 7.79 (d, *J* = 8Hz, 1H), 7.70 (m, 1H), 7.55 (m, 1H), 7.31 (t, *J* = 8Hz, 1H), 4.46 (t, *J* = 8 Hz, 2H), 1.77 (m, 2H), 1.25 (m, 6H) and 0.87 (t, *J* = 8 Hz, 3H).

^{13}CNMR (100 MHz, DMSO-d_6) δ (ppm): 13.7, 22, 26, 28.4, 30.9, 42.5, 109.7, 110.2, 120, 120.7, 122.11, 122.2, 124, 126.6, 126.7, 128.2, 140.4, 142.6 and 192.

2.3.6. Synthesis of 5-[6-(4,6-dioxo-2-thioxohexahydro-5-pyrimidinylidenmethyl)-9-butyl-9H-3-carbazolylmethylene]-2-thioxohexahydro-4,6-pyrimidinedione (DTB-CB)

In a dried 100 ml, round bottom flask N-butylcarbazole-3,6-dicarbaldehyde (0.28 g, 1 mmol) and thiobarbituric acid (0.29 g, 2 mmol) were dissolved in absolute ethanol (3 mL). After heating the reaction mixture for 5 h, the bright red dye was obtained and filtered, washed with 30 ml water three times. The dye BD-CH obtained was purified by crystallization from EtOAc/n-hexane.

Dark red powder, Yield: 82% .
FT-IR (KBr/cm^{-1}): 3419, 3202, 3066.26, 2958, 1665, 1524, 1483, 1376, 1287, 1242, 1167 and 1027.

^{1}HNMR (400 MHz, DMSO-d_6) δ (ppm): 12.44 (s, 1H), 11.81 (s, 1H), 9.33 (s, 2H), 8.51 (d, *J* = 4, 2H), 7,80 (s, 2H), 7.28 (d, *J* = 8 Hz, 2H), 4.50 (t, *J* = 6, 2H), 1.77 (m, 2H), 1.29 (m, 2H), 0.9 (t, *J* = 8, 3H).

^{13}CNMR (100 MHz, DMSO-d_6) δ (ppm): 178.2, 163, 160, 157.3, 144, 134.5, 128.8, 125, 122.5, 115,110, 43, 30.5, 19.5 and 13.5. Mass: m/z 532 (M+1), 529, 523, 503, 479,444 and 430.

Anal. Calcd. for $C_{26}H_{21}N_5O_4S_2$ (531.10): C, 58.74; H, 3.98; N, 13.17, Found: C, 58.72; H, 3.99; N, 13.16.

2.3.7. Synthesis of 5-(9-Hexyl-9H-carbazol-3-ylmethylene)-2-thioxo-dihydro-pyrimidine-4,6-dione (TB-CH)

In a dried 100 ml, round bottom flask 9-Hexyl-9H-carbazole-3-carbaldehyde (0.28 g, 1 mmol) and thiobarbituric acid (0.15 g, 1 mmol) were dissolved in absolute ethanol (3 mL). After heating the reaction mixture for 5 h, the bright red dye was obtained and filtered, washed with 30 ml water three times. The dye BD-CH obtained was purified by crystallization from EtOAc/n-hexane.

Orange powder, Yield: 75% .

FT-IR (KBr/cm^{-1}): 3411, 3154, 2159, 1661, 1514, 1463, 1389, 1290, 1187 and 1067.

^{1}HNMR (400 MHz, DMSO-d_6) δ (ppm): 12.41 (s, 1H), 12.32 (s, 1H), 9.35 (s, 1H), 8.37 (d, *J* = 8, 2H), 8.54 (s,1H), 8.18 (d, *J* = 8, 2H), 7.71(m, 2H), 7.54 (t, *J* = 8 1H), 7.33 (t, *J* = 8, 1H), 4.45 (t, *J* = 8, 2H), 3.53 (m, 2H), 2.51(m, 2H), 1.77 (m, 2H), 1.24(m, 2H), 0.79 (t, *J* = 8, 3H).

^{13}CNMR (100 MHz, DMSO-d_6) δ (ppm): 178.1, 162.5, 160, 158, 143.5, 141, 134, 130, 127, 123.5, 122.5, 121, 114, 110, 109, 43, 31, 30.5, 28.5, 26, 26.5, 22 and 14.

Mass: m/z 406 (M+1), 389, 360, 334, 232 and 204.

Anal. Calcd. for $C_{23}H_{23}N_3O_2S$ (405.15): C, 68.16; H, 5.72; N, 10.76, Found: C, 68.15; H, 5.70; N, 10.75.

2.3.8. Synthesis of 5-(9-Butyl-9H-carbazol-3-ylmethylene)-2-thioxo-dihydro-pyrimidine-4,6-dione (TB-CB)

In a dried 100 ml, round bottom flask 9-Butyl-9H-carbazole-3-carbaldehyde (0.25 g, 1 mmol) and thiobarbituric acid (0.15g, 1 mmol) were dissolved in absolute ethanol (3 mL). After heating

the reaction mixture for 5 h, the bright red dye was obtained and filtered, washed with 30 ml water three times. The dye BD-CH obtained was purified by crystallization from EtOAc/n-hexane.

Orange powder, Yield: 78%.

FT-IR (KBr/cm^{-1}): 3407, 3122, 2924, 2856, 1649, 1598, 1513, 1494, 1386, 1301, 1190 and 1063.

^{1}HNMR (400 MHz, DMSO-d_6) δ (ppm): 12.42 (s, 1H), 12.33 (s, 1H), 9.34 (s, 1H), 8.67 (d, *J*= 8, 2H), 8.50 (s,1H), 8.18 (d, *J* = 8, 2H), 7.71(m, 2H), 7.54 (t, *J* = 8 1H), 7.32 (t, *J* = 8, 1H), 4.50 (t, *J* = 8, 2H), 1.77 (m, 2H), 1.29(m, 2H), 0.80 (t, *J* = 8, 3H).

^{13}CNMR (100 MHz, DMSO-d_6) δ (ppm): 191.7, 178, 162.5, 160, 158, 143, 140.6, 133.7, 130.2, 127, 125, 123.5, 122.5, 120, 114, 110.5, 109.5, 42.5, 30.5, 19.5 and 13.5.

Mass: m/z 388 (M+1), 334, 261, 204, 190and 176.

Anal. Calcd. for $C_{21}H_{19}N_3O_2S$ (377.12): C, 68.82; H,5.07; N, 11.13, Found: C, 68.78; H, 5.05; N, 11.10.

3. Computational details

To theoretically understand the donor effects and the sensitized mechanism at a molecular level, the geometric and electronic structures of dyes were studied in detail using DFT calculations of dyes by Gaussian 03 package. The geometries of BD-CH, BTD-CH and DT-CH were optimized by using the B3LYP method with the 6-31 G (d) basis set. Salvation effects were introduced by the SCRF method, via the conductor polarizable continuum model (CPCM) implemented in the Gaussian program, for both geometry optimizations and TD-DFT calculations. To model the adsorption modes of the dyes on the TiO_2 anatase(101) surface, periodic density functional theory calculations were carried out using the Dmol^3 package as implemented in Material Studio (version 5.5). The TiO_2 anatase (101) surface is modeled using a slab with a thickness of six atomic layers. Periodic boundary conditions are employed with a surface super cell of 21.77 × 15.10 $A^{\circ 2}$ and a vacuum layer of at least 20 A° to prevent interaction between adjacent slabs. For these calculations, we used the generalized gradient approximation (GGA) functional with Perdew and Wang (PW91) formulation. The electronic properties of core electrons were treated with DFT semi-core pseudoplots in term of the DNP basis set. The convergence energy

tolerance, gradient, and displacement convergence were 1.0×10^{-5} Ha, 0.004 Ha $A^{\circ -1}$, and 0.005 respectively.

4. Results and discussion

4.1. Synthesis strategy

Dye molecules have an essential role in DSSC performance; the capability of solar cell in sun power harnessing depends to dye structure. Molecular designs for organic sensitizers are very flexible. Therefore; to achieve dyes contain thiobarbutiric acid as anchoring group, and study the potential of them for application in solar cell, TB-CH, TB-CB and BTD-CB dyes were synthesized in three-step reactions that is shown in Scheme 2. First by the reaction of carbazole and hexylbromide or butylbromide in the presence of NaOH in DMSO as solvent, 9-Hexyl-9H-carbazole and 9-butyl-9H-carbazole were synthesized. The yield of reaction was satisfactory and was about 85%. In the next step by application of Vilsmeier–Haack reaction, alkyl-carbazole was formylated. For this purpose, 9-hexyl-9H-carbazole and 9-butyl-9H-carbazole reacted with $POCl_3$ in the presence of DMF as the reagent and solvent. The yield of this reaction was 60%. In the final step corresponding carbaldehyde reacted with thiobarbutiric acid via Knoevenagel condensation. Synthesis of TB-CH, TB-CB and DTB-CB was carried out in the presences of ethanol without using any basic catalyst. The yields of reactions were 86, 82, and 88%, respectively. The synthesis of TB-CH, TB-CB and BTD-CB dyes was confirmed by IR and ^{1}HNMR, ^{13}CNMR, mass spectroscopy and CHN analysis.

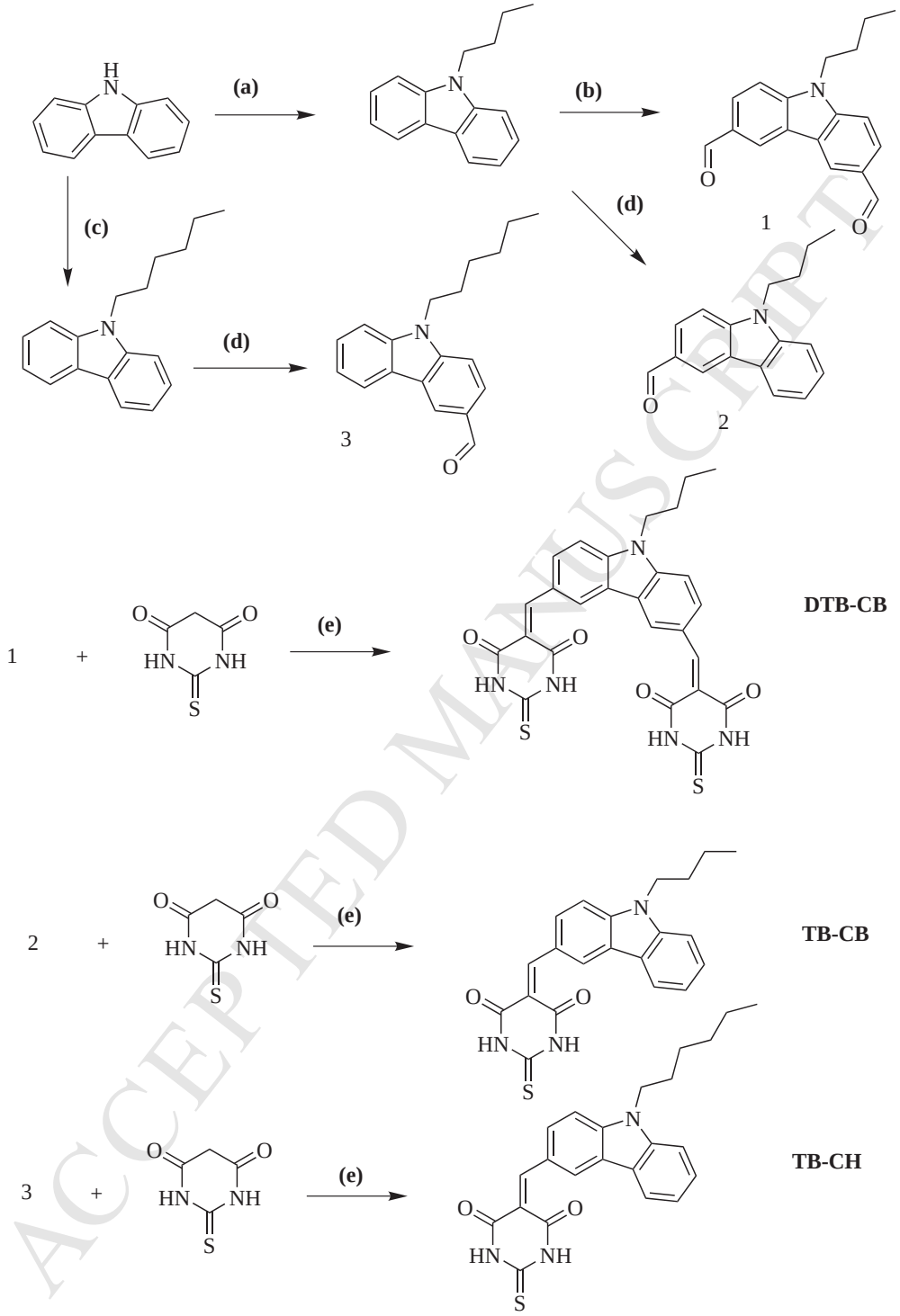

Figure 2. Synthetic routes of TB-CH, TB-CB and DTB-CB (a) 1-Bromohexyl, NaOH, DMSO, 110℃, overnight (b) $POCl_3$, DMF, 95℃, overnight (c) 1-Bromobutyl, NaOH, DMSO, 110℃, overnight (d) $POCl_3$, DMF, 95℃, 5 h (e) Ethanol, 55℃, 5 h.

4.2. Photo physical characterization by UV–Vis absorption spectra of dyes

UV–Vis analysis is a useful method for evaluation of sun power harnessing capability of dyes [25]. In order to study dye structure in function of light harvesting, we measured the absorption spectra of the dyes in THF solution and at a monolayer of adsorbed dyes on the TiO_2 film. The absorption spectra of dyes (TB-CH, TB-CB and DTB-CB) in THF solution at a concentration of 3×10^{-4} M have shown in Figure. 3, and data are listed in Table 1. All dyes showed broad absorption spectra in the visible region. Generally, absorption bands at around 300 nm are related to π-π electron transition. The λ_{max} of TB-CH, TB-CB and DTB-CB on the film was 456, 457 and 475, respectively. The result revealed that length of alky group in dye structure has not significant effect on the absorption bands. It is notable DTB-CB contains two acceptor unit and therefor shows higher λ_{max} in comparison to TB-CH and TB-CB. Also, fluorescence emission was recorded in THF and spectra are displayed in figure 4. The λ_{ex} of TB-CH, TB-CB and DTB-CB was 456, 457 and 475 nm, respectively. In addition, the fluorescent intensity of TB-CH, TB-CB and DTB-CB was 3.44, 3.77 and 8.01 respectively. The maximum emission of TB-CB is shifted toward the longer-wavelength region. It is due to the presence of butyl moiety in its structure. DTB-CB emission is shifted toward the lower-wavelength region. This observation may be due to the presence of second group of thiobarbutiric acid as the anchoring part and higher resonance in DTB-CB molecule.

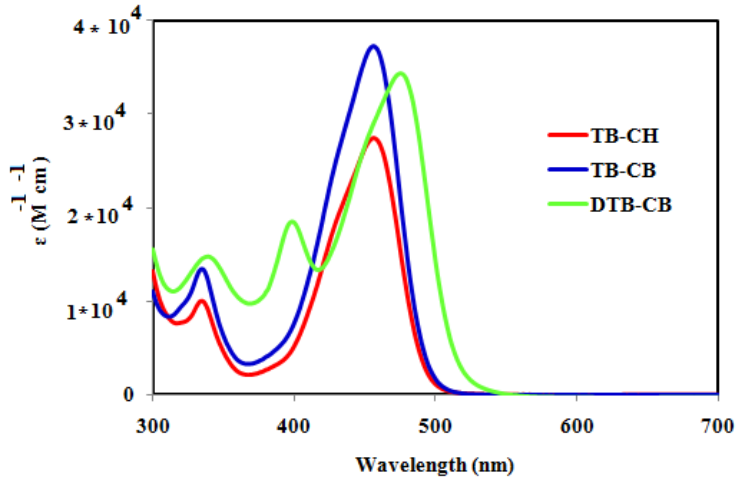

Figure 3. Absorption spectra of dyes TB-CH, TB-CB and DTB-CB in THF.

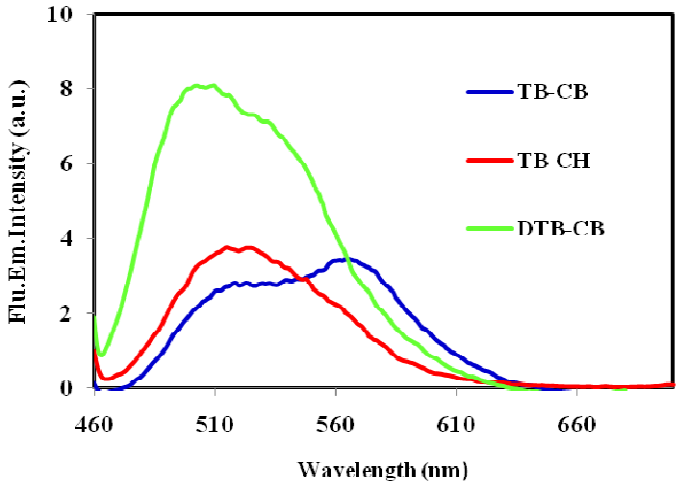

Figure 4. Emission spectra of dyes TB-CH, TB-CB and DTB-CB in THF λex = 456,457 and 475 nm; Conc= 10^{-5} M.

In order to monitor the photophysical properties, Absorption spectral of dyes TB-CH, TB-CB and DTB-CB on TiO_2 film is presented in Figure 5. DTB-CB shows higher absorbance near 370 nm, but near 470 nm its absorption decrease significantly. Two other dyes represent smoother absorption by little changes around 370 and 470 nm.

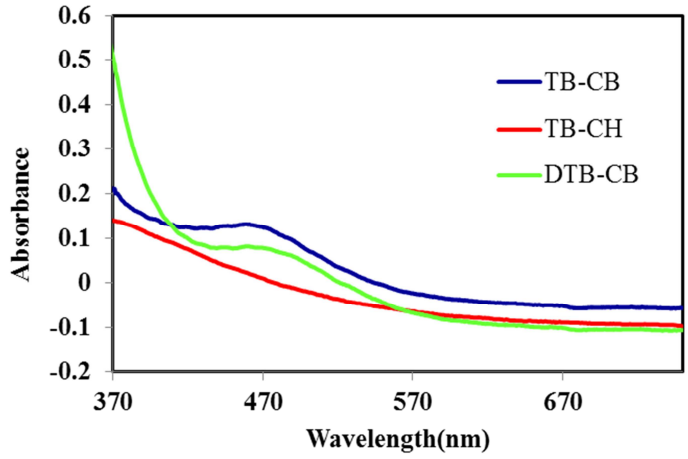

Figure 5. Absorption spectral of dyes TB-CH, TB-CB and DTB-CB on TiO_2 film.

4.3 Electrochemical properties of dyes

One way to study of electrochemical properties is evaluation of LUMO and HOMO levels of dyes molecules. LUMO and HOMO levels of dyes must be suitable to match the conduction

band (E_{cb}) of TiO_2 electrode and the HOMO level of I_3^-/I^-, respectively. E_{cb} of TiO_2 electrode must be more positive than LUMO of dye molecules for the injection of electrons, and for accepting electron, the level of I^-_3/I^- must be more negative than the HOMO level of dye molecules, and regenerate from the oxidized state [26].

Table 1. Band gap (calculated by DFT/B3LYP), absorption, and electrochemical parameters for organic dyes.

parameter	TB-CH	TB-CB	DTB-CB
UV (λ_{max}/nm)[a]	370	370	370
UV (λ_{max}/nm)[b]	456	457	475
Oxidation (V vs. NHE) [c]	1.5	1	1.2
Reduction (V vs. NHE)[d]	-0.95	-1.47	-1.13
$E_{0\text{-}0}$[e]	2.45	2.47	2.33
(HOMO/LUMO) (ev)[f]	-0.24/ -0.30	-0.09 / -0.21	-0.25/ -0.30
Band gap[f]	0.6	0.12	0.5

[a] Maximum absorption on TiO_2 film.

[b] Maximum absorption in THF.

[c] Oxidation of dyes measured by cyclic voltammetry in 0.1 M Bu_4NPF_6 in THF solution as supporting electrolyte, Ag/AgCl as reference electrode and Pt as counter electrode. Potentials measured vs Ag/AgCl was converted to normal hydrogen electrode (NHE) by addition of +0.2V

[d] Reduction was calculated by HOMO–$E_{0–0}$.

[e] $E_{0–0}$ transition energy measured at the onset of absorption spectra.

[f] DFT/B3LYP calculated values

Therefore, the electrochemical properties of dyes were studied to explain their HOMO and LUMO levels. Potentials measured vs Ag/AgCl was converted to normal hydrogen electrode (NHE) by addition of +0.2 V.

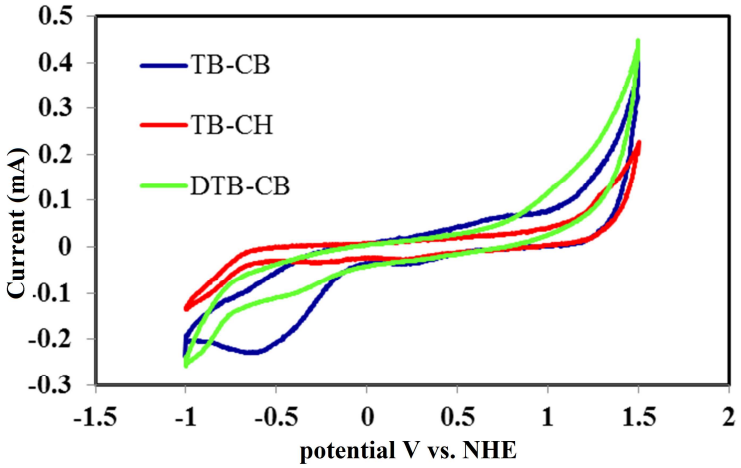

Figure 6. CVs of the TB-CH, TB-CB and DTB-CB dye films in DMF containing 0.1 M Bu_4NPF_6 at a scan rate of 100 mVs^{-1}, vs Ag/AgCl**.**

As shown in Figure. 6, the HOMO levels of TB-CH, TB-CB and DTB-CB are 1.5, 1 and 1.2 V (vs. NHE) respectively. In comparison to I_3^-/I^-, redox potential value of dyes showed higher oxidative potential levels, indicating that the oxidized dyes formed after electron injection to the TiO_2 and therefore could accept electrons from iodide ions thermodynamically. Results revealed that the longer alkyl group caused higher HOMO level and also DTB-CB by having two acceptor units has higher HOMO level potential in comparison with TB-CB. On the other hand, the LUMO level of TB-CH, TB-CB, and DTB-CB are -0.95, -1.47, -1.13 (vs. NHE), respectively, which all are more negative than the conduction-band edge of the TiO_2. Furthermore; band gaps were 2.45, 2.47 and 2.33 eV for the BD-CH, BTD-CH and DT-CH, respectably. These results clarify that the dyes are potentially efficient sensitizer for dye synthesized solar cells. The schematic energy levels of TB-CH, TB-CB and DTB-CB based on absorption and electrochemical data are shown in Figure. 7.

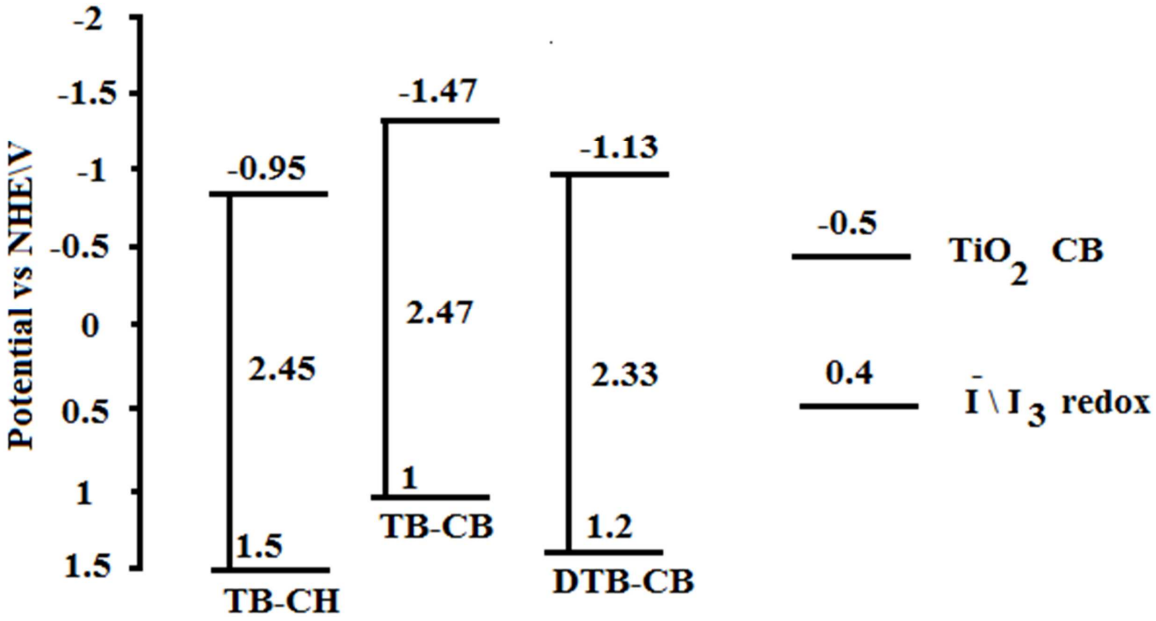

Figure 7. Schematic energy levels of TB-CH, TB-CB and DTB-CB based on absorption and electrochemical data.

4.4. Molecular electrostatic potential, dipole moments and polarizability of dyes

Total charge distribution of a molecule at a point in space around the molecule produce net electrostatic effect. This phenomenon is known as molecular electrostatic potential (ESP). Electrostatic potential is related to the total charge distribution with dipole moments, partial charges, electronegativity and site of chemical reactivity of a molecule. It provides a way to visualize the relative polarity of a molecule. The different values of the electrostatic potential at surface are represented by different colors; potential increases in the order blue > green > yellow > orange > red. Electrostatic potential maps of TB-CH, TB-CB, and DTB-CB are presented in Figure. 8. Dipole moment and polarizability are very important physical quantities of dye molecules in DSSCs [28]. Molecular electrostatic potential calculations were performed in order to analyze the charge populations of TB-CH, TB-CB and DTB-CB. In this work, the electron donor units of the dyes are hexyl and butyl moieties. As presented in Figure. 8 electrostatic potential of dyes were mostly over alkyl groups and π bridge (carbazole).

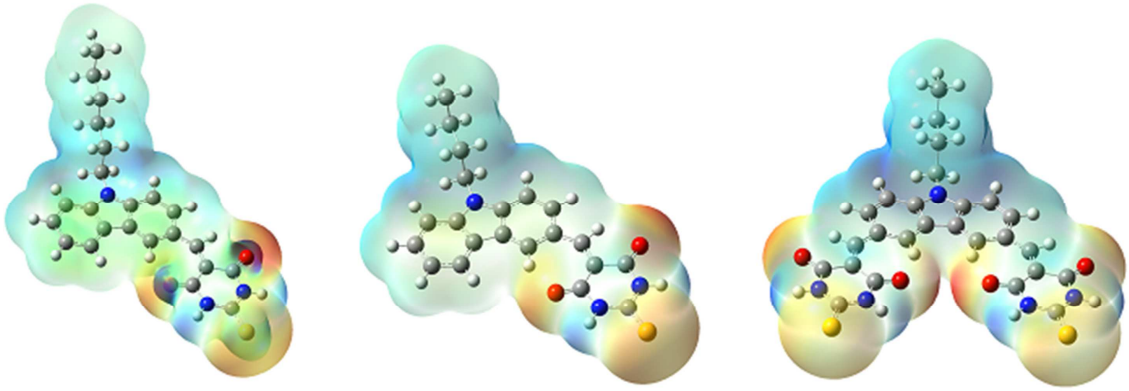

TB-CH **TB-CB** **DTB-CB**

Figure. 8 Molecular electrostatic potential mapped on the isodensity surface of TB-CH, TB-CB and DTB-CB

4.5. Frontier molecular orbitals of dyes and intramolecular electron transfer

To get further insights into the molecular structure and electronic distribution of these organic dyes, we performed a molecular orbital analysis (MOA). The frontier molecular orbital contribution is very important in determining the charge-separated states of dye sensitizers [24]. Oxidation potential of dye sensitizer is directly related to the highest occupied MO (HOMO) level and driving force for the reduction of oxidized dye increase at the larger oxidation potential. In a solar cell, the dye molecule absorbs light energy, and it injects an electron into the LUMO of the dye molecule, and then ultimately injects it into the conduction band of TiO_2. The electron distribution of the HOMO and LUMO of TB-CH, TB-CB and DTB-CB are shown in Figure. 9. The HOMO and LUMO energies, as well as the HOMO-LUMO gaps (Eg) of TB-CH, TB-CB and DTB-CB are listed in Table 1. As indicated from the Figure. 9, the HOMO is delocalized over the entire thiobarbutiric acid ring, especially S atom. In the LUMO orbital, the electron density has shifted toward the carbazole as π bridge and acceptor end of the molecule. The band gap for TB-CH, TB-CB and DTB-CB is 0.6, 1.2 and 0.5 eV respectively. Due to the position of LUMO connected to the acceptor group, therefore, the dyes can give suitable electron injection from their LUMO orbitals to TiO_2 conduction band [28], so the dyes would show the satisfactory solar cell efficiency as a result of good absorption characteristics.

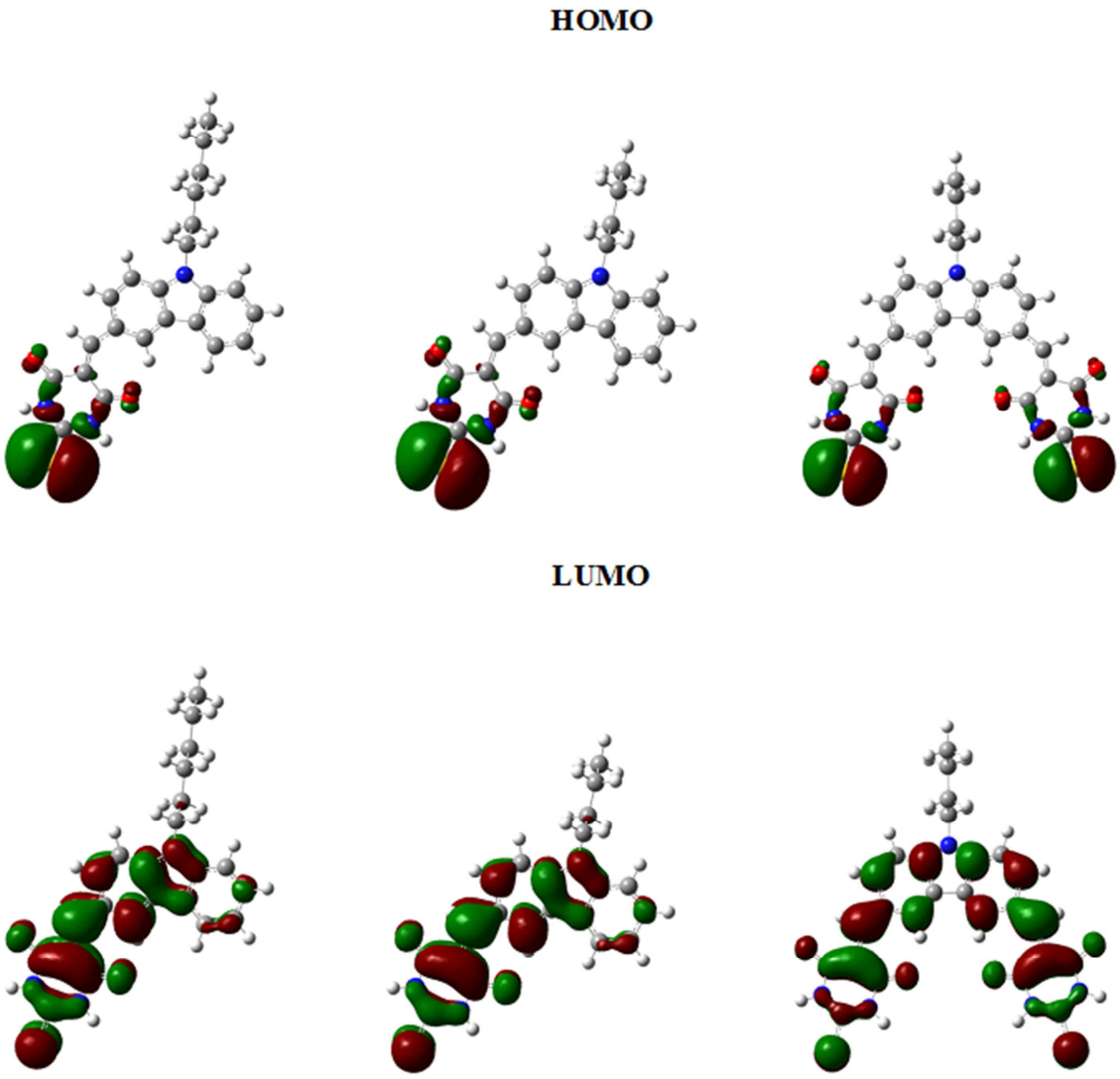

Figure 9. The frontier molecular orbitals of the HOMO and LUMO levels calculated with B3LYP/6-31G (d) of the synthesized dyes.

4.6. Optic absorption properties of dyes

In order to understand electronic transitions of TB-CH, TB-CB and DTB-CB; calculations of absorption spectra in THF were done by the time-dependent (TD) method on the optimized geometries. The comparison UV-Vis absorption of TB-CH, TB-CB and DTB-CB based on calculation and experiments are presented in Table 3. Calculations showed that the visible absorption maxima of this kind of dyes correspond to the electron transition from HOMO to LUMO. The λ_{max} is a function of the electron availability. It is due to electronic transition from

carbazole ring, and acceptor unit (transition of π–π* type). The observed and computed absorption maxima are in agreement.

Table 3. EIS parameters obtained from modelling the EIS result.

Compound	λ_{cal} (nm)[a]	λ_{obs} (nm)[b]
TB-CH	452.37	456
TB-CB	452.50	457
DTB-CB	477.95	475

[a]Visible absorption maxima calculated by DFT

[b]The observed visible absorption

4.7 Adsorption of dyes on TiO_2 anatase (101) surface

The optimized geometries of dye/TiO_2 systems are shown in Figure. 10 and the corresponding bond distances as well as adsorption energies are provided in Table 4. As shown in Table 4, all the dyes show a rather strong adsorption onto the TiO_2 surface, with binding distances of 2.69, 2.69, and 2.86–2.68 Aº for TB-CH, TB-CB, and DTB-CB, respectively. The adsorption energy, E_{ads} is calculated using the following expression

$E_{ads} = E_{(slab+dye)} - E_{slab} - E_{dye}$

Where E_{slab} represents the energy of the clean slab, E_{dye} represents the anchored dye in the gas phase, and $E_{(slab+dye)}$ is the total energy of the complex of the slab with anchored dye. A negative value of E_{ads} indicates stable adsorption. As shown in Table 4, the adsorption energy (E_{ads}) of each dye/TiO_2 complex was calculated to be -1.05, -1.01 and -1.00 eV for TB-CH, TB-CB and DTB-CB, respectively, which are sufficiently large to allow the assumption that the dye molecules are chemisorbed on the surface of TiO_2. The HOMOs and LUMOs of dye–TiO_2 complexes were also studied. Fig. 10 shows the electron density distribution in the systems, TB-CH, TB-CB and DTB-CB. The electron density distribution in the HOMOs and LUMOs of these three dye@TiO_2 systems showed no reasonable deviation. In the case of HOMOs of DTB-CB, despite the presence of two thiobarbituric rings, the electron density was localized mainly over one thiobarbituric ring attached directly to the TiO_2. On the contrary, TB-CH, TB-CB presents HOMOs that are delocalized throughout the organic molecule.

On the other hand, in the case of the LUMOs, the electron density was shifted completely to the TiO_2. The shifting of the electron density from the dye to the TiO_2 indicates the direct electron injection process from the excited state of the dye to the conduction band of TiO_2.

Table 4. Selected bond lengths (Aº) and adsorption energies (eV) of dye/TiO_2 systems.

	Ti–S (ºA)	**Ti–S (ºA)**	E_{ads} **(eV)**
TB-CH	2.693	-	-1.05
TB-CB	2.686	-	-1.01
DTB-CB	2.864	2.684	-1.00

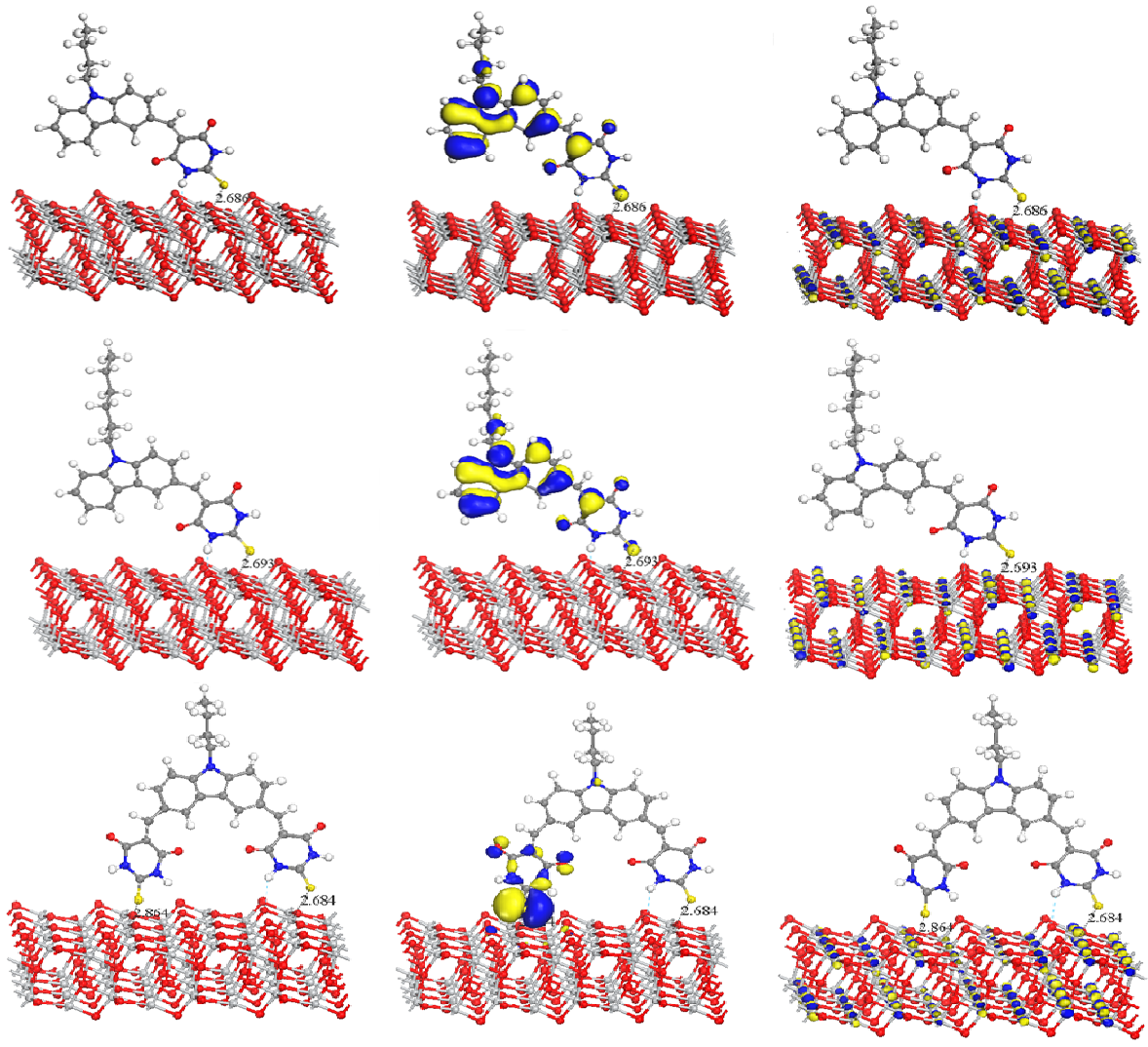

Figure 10. Frontier orbitals of the dye–TiO_2 complexes.

5. Conclusion

In the present work, we designed and synthesized TB-CH, TB-CB and DTB-CB organic dyes. Also we evaluated the electronic and polarizabilities of them by DFT method. The electronic absorption properties were investigated using TD-DFT. Generally, the present theoretical results agree with the experimental results. Polarizabilities applied in order to study the anchoring properties of synthesized dyes and the efficiency of electron injection to TiO_2. Also, the light harvesting abilities of the dyes have been studied by investigation of electronic structures. The polarizability suggests that the charges of similar acceptors in different dyes are very similar. The longer alkenyl in conjugate bridge result in the higher HOMO energy, and then induce higher driving force for the reduction of oxidized dyes. The introducing two acceptors in DTB-CB stabilized the HOMO and LUMO, and reduce the Eg. The absorption properties based on experiments and calculations indicate that the, DTB-CB has higher absorption in UV-Vis region. In evaluation of anchoring properties, absorption spectral of dyes on TiO_2 film is important. Results indicate all dyes show week absorption especially TB-CH. This malfunction may be duo to large size ring, presence of sulfur atom simultaneously. Adsorption energy is one of the factors to determine dye efficiency for solar cells theoretically, dyes have higher adsorption energy have better function and higher light harvesting in solar cell [23, 27]. By the result of absorption dyes on TiO_2 film and adsorption energy; dyes contain thiobarbutiric acid moiety as an electron acceptor are not prone to produce high efficiency in solar cells. But application of carbazole and alkyl groups as bridge and donor moiety is suggested.

Acknowledgments

We are grateful to the Yasouj University and Sharif Univercity of technology, Iran, for financial supports.

References

1. Y. A. Tayade, D. R. Patil, Y. B. Wagh, A. D. Jangle, D. S. Dalal, An efficient synthesis of 3-indolyl-3-hydroxy oxindoles and 3,3-di(indolyl)indolin-2-ones catalyzed by

sulfonated β-CD as a supramolecular catalyst in water, Tetrahedron Lett. 56 (2015) 666-673.

2. M. Grätzel, Photoelectrochemical cells, Nature 414 (2001) 338-344.
3. Q. Huaulmé, E. Cece, A. Mirloup, R. Ziessel, Star-shaped panchromatic absorbing dyes based on a triazatruxene platform with diketopyrrolopyrrole and boron dipyrromethene substituents, Tetrahedron Lett. 55 (2014) 4953-4958.
4. A. Hagfeldt, G. Boschloo, L. Sun, L. Kloo, H. Pettersson, Dye-sensitized solar cells, Chem. Rev. 110 (2010) 6595-6663.
5. L. Giribabu, V. K. Singh, M. Srinivasu, C. V. Kumar, V. G. Reddy, Y. Soujnya, P. Y. Reddy, Synthesis and photoelectrochemical characterization of a high molar extinction coefficient heteroleptic ruthenium(II) complex, J. Chem. Sci. 123 (2011) 371-378.
6. C. Satheeshkumar, M. Ravivarma, P. Rajakumar, R. Ashokkumar, D. C. Jeong, C. Song Synthesis, photophysical and electrochemical properties of stilbenoid dendrimers with phenothiazine surface group, Tetrahedron Lett. 56 (2015) 321-326.
7. M. K. Nazeeruddin, C. Klein, P. Liska, M. Gratzel, Synthesis of novel ruthenium sensitizers and their application in dye-sensitized solar cells, Coord. Chem. Rev. 249 (2005)1460-1467.
8. M. K. Nazeeruddin, F. D. Angelis, S. Fantacci, A. Selloni, G. Viscardi, P. Liska, S. Ito, B. Takeru, M. Grätzel, Combined experimental and DFT-TDDFT computational study of photo electrochemical cell ruthenium sensitizers, J. Am. Chem. Soc. 127 (2005) 16835-16847.
9. K. Yung Teo, M. Hing Tiong, H. Yee Wee, N. Jasin, Z-Q. Li, M. Yang Shiu, J. Yang Tang, J-K. Tsai, R. Rahamathullah, W. M. Khairul, M.Guan Tay, The influence of the push-pull effect and a π-conjugated system in conversion efficiency of bis-chalcone compounds in a dye sensitized solar cell, J. Mol. Struct. 1143 (2017) 42-48.
10. I.N. Obotowoa, I.B. Obotb, U.J. Ekpe, Organic sensitizers for dye-sensitized solar cell (DSSC): Properties from computation, progress and future perspectives, J. Mol. Struct. 1122 (2016) 80-87.

11. A. G. Al-Sehemi, A. Irfana, A. M. Asiri, Y. Ahmed Ammar, Molecular design of new hydrazone dyes for dye-sensitized solar cells: Synthesis, characterization and DFT study, J. Mol. Struct. 1019 (2012) 130-134.

12. B. Liu, W. Q. Li, B. Wang, X. Y. Li, Q. B. Liu, Y. Naruta, W. H. Zhu, Influence of different anchoring groups in indoline dyes for dye-sensitized solar cells: Electron injection, impedance and charge recombination, J. Power Sources 234 (2013)139-146.

13. Z. Iqbal, W. Q. Wu, D. B. Kuang, L. Y. Wang, H. Meier, D. R. Cao, Phenothiazine-based dyes with bilateral extension of π-conjugation for efficient dye-sensitized solar cells, J. Dyes Pigments 96 (2013) 722-731.

14. Q. Xie, J. Zhou , J. Hu , D. Peng , Y. Liu, Y. Liaong , C. Zhu , C. Zhong, Synthesis and Photovoltaic properties of branched chain polymeric metal complexes containing Phenothiazine and Thiophene derivative for dye-sensitized solar cells, J. Chem. Sci. 127 (2015) 395-403.

15. Y. Z. Wu, W. H. Zhu, Organic sensitizers from D–π–A to D–A–π–A: effect of the internal electron-withdrawing units on molecular absorption, energy levels and photovoltaic performances, Chem. Soc. Rev. 42 (2013) 2039-2045.

16. S. Jungsuttiwong, R. Tarsang, T. Sudyoadsuk, V. Promarak, P. Khongpracha, S. Namuangruk, Theoretical study on novel double donor-based dyes used in high efficient dye-sensitized solar cells: The application of TDDFT study to the electron injection process, Org. Electron. 14 (2013) 711-722.

17. A. G. Al-Sehemia, A. Irfan, A. M. Asiri, Y. A. Ammar, Molecular design of new hydrazone dyes for dye-sensitized solar cells: Synthesis, characterization and DFT study, J. Mol. Struct. 1019 (2012) 130-134.

18. J. J. Guo, S. R. Wang, X. G. Li, F. Zhang, X. Shao Na, X. J. Lian, The synthesis, molecular structure and photophysical properties of 2, 9, 16, 23-tetrakis (7-coumarinoxy-4-methyl)-phthalocyanine sensitizer, J. Mol. Struct. 1060 (2014) 17-28.

19. U. Diebold, The surface science of titanium dioxide, Surf. Sci. Rep. 48(2003)53-229.

20. A. Najafi Chermahini, H. Farrokhpour, A. Zeinodini, Adsorption of some important tautomers of 5-amino tetrazole on the (001) and (101) surfaces of anatase: Theoretical study, J. Mol. Struct. 1121 (2016) 203-214.
21. K. Eun Lee, M.A. Gomez, S. Elouatik, G. P. Demopoulos, Further Understanding of the Adsorption Mechanism of N719 Sensitizer on Anatase TiO_2 Films for DSSC Applications Using Vibrational Spectroscopy and Confocal Raman Imaging, Langmuir, 26 (2010) 9575-9583.
22. A.Najafi Chermahini, B. Hosseinzadeh, A. Salimi Beni, A. Teimouri, M. Moradi, A periodic density functional theory study of tetrazole adsorption on anatase surfaces: potential application of tetrazole ring in dye-sensitized solar cells, J. Mol. Model. 20 (2014) 2086-2096.
23. B. Hosseinzadeh, A. Salimi Beni, M. Azari, M. Zarandi, M. Karami, Novel D–π–A type triphenylamine based chromogens for DSSC: design, synthesis and performance studies, New J. Chem.40 (2016) 8371-8382.
24. M. Zarandi, A. Salimi Beni, Synthesis and DFT calculation on novel derivatives of Bis (indolyl) methanes, J. Mol. Struct. 1119 (2016) 404-412.
25. J. Xu, L. Wang, L. Liu, Z. Bai, L. Wang, G. Liang, X. Shen, W. Xu, A theoretical investigation of tetrahydroquinoline dyes with different spacers used for sensitized solar cells, Can. J. Chem. 89 (2011) 978-986.
26. V. Barone, M. Cossi, Quantum Calculation of Molecular Energies and Energy Gradients in Solution by a Conductor Solvent Mode, J. Phys. Chem. A 102 (1998) 1995-2001.
27. B. Hosseinzadeh, A. Salimi Beni, A. Najafi Chermahini, R. Ghahary, A. Teimouri, Novel organic dyes with anchoring group of barbituric/thiobarbituric acid and their application in dye-sensitized solar cells, Synthetic Met. 209 (2015) 1-10.

Highlights

I. We applied carbazole base as π bridge unit in all synthesis dyes

II. 3 novel dyes synthesized and the structure of dyes studied

III. Dyes were investigated by UV spectroscopy and cyclic voltammetry (CV)